

Internal tides in the waters surrounding the Faroe Plateau

Karin Margretha H. Larsen, Bogi Hansen, Regin Kristiansen, and Svein Østerhus

ABSTRACT

In the period 1994 - 1999, long-term current measurements have been acquired from several sites around the Faroe Plateau from moored, upward-looking ADCP's. They provide a detailed description of the vertical current profiles which allows an overview of the changes in tidal current with depth. The waters surrounding the Plateau have a pronounced baroclinic density structure, and the observations demonstrate the existence of pronounced internal tides. Harmonic constants determined from repeated measurements at the same sites vary more than can be explained by instrumental or analytical inaccuracy, indicating non-stationary tidal characteristics. In spite of this, the semidiurnal constituents exhibit a fairly consistent and simple behaviour which may be described as a two-layer system with a continuous change from the upper to the deeper layer and with a very diminished semidiurnal tide in the deep parts of the Faroe Bank Channel. The diurnal tides have a more complicated depth variation.

Karin Margretha H. Larsen, Bogi Hansen, and Regin Kristiansen: Faroese Fisheries Laboratory, P.O.Box 3051, FO-110 Torshavn, Faroe Islands, email: karinl@frs.fo, bogihan@frs.fo, regink@frs.fo. Svein Østerhus: Geophysical Institute, Allegaten 70, N-5007 Bergen, Norway, email: svein@gf.uib.no

INTRODUCTION

The Faroe Plateau (Fig. 1) is surrounded by waters that are highly stratified in most areas. The upper layers are dominated by the relatively warm and saline Atlantic water flowing into the Norwegian Sea. The deeper layers, on the other hand, are in most areas much colder and somewhat less saline due to their origin by thermohaline sinking in the Arctic Mediterranean (Arctic Ocean and Nordic Seas). A pronounced pycnocline is therefore found at depths of 400 - 600 m all around the Plateau except for the area northwest of the Plateau which is in the Atlantic.

This fact implies that internal motions may be expected, and already Knudsen (1911) was able to verify that indeed there were large vertical excursions of isotherms at mid-depth in the Faroe-Shetland Channel. He based his discussion mainly on a series of continuous observations during 67 hours at one station in the channel. At this station, the pycnocline was close to the 400 m level and at this depth, vertical excursions were found to exceed a 100 m and a clear periodicity was established with mainly semi-diurnal, but also some diurnal, influence.

As noted by Sherwin (1995), Knudsen was not the only one in his time to consider this an important phenomenon, but, with a few exceptions, later investigators have not focused very much on internal tides in the Faroe-Shetland Channel. As for the rest of the waters surrounding the Faroe Plateau, even less is known, and we do not have a comprehensive overview over the internal tide in the area. This is a pity, because tides, both barotropic and internal, are among the most easily predictable marine phenomena and several species of fish prefer the temperatures found in the thermocline. It is conceivable that the distribution of these species varies with the internal tide in a predictable manner. For pelagic fish, variations of vertical distribution will be of most interest, but also the horizontal distribution of demersal fish species may be affected by a periodic variation of the bottom temperature in the slope region.

This is mainly a phenomenological study. We do not attempt a theoretically founded explanation of the pycnocline motion and baroclinic velocity variations. Rather, we use observations acquired for other purposes to get an indication of the magnitude and predictability of the internal tide around the Faroe Plateau in order to gain empirical knowledge and evaluate whether further studies would be relevant.

DATA MATERIAL

We use two main sets of observations: CTD-data and data from moored ADCP's (Acoustic Doppler Current Profilers).

Table 1. Main characteristics of the CTD standard sections considered. For each section (Fig. 2) the table lists start and end position and number of standard stations included. It also lists the period and the number of cruises with complete temperature and salinity distribution on the section.

Section	Start position	End position	Standard stations	Period	Complete TS sections
N	62°20'N 6°05'W	63°50'N 6°05'W	10	1987-1999	42
E	62°00'N 6°12'W	61°28'N 3°42'W	8	1988-1999	35
S	61°16'N 6°38'W	60°35'N 4°45'W	8	1994-1999	22
V	61°50'N 7°00'W	61°20'N 7°53'W	6	1988-1999	45

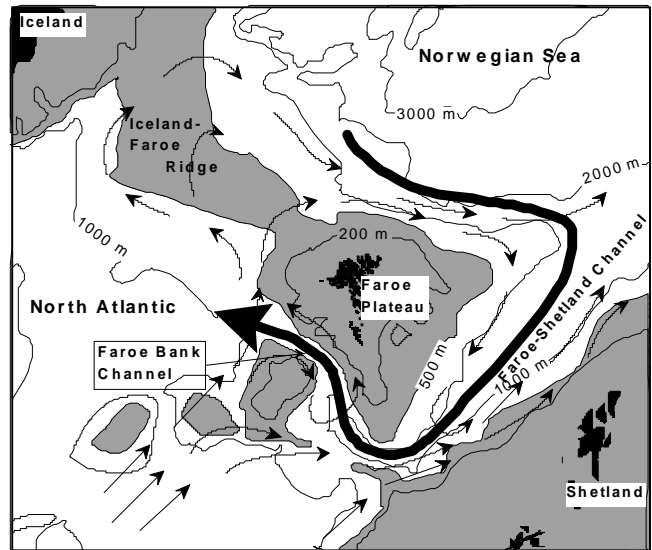


Figure 1. The Faroe Plateau is situated on the Greenland-Scotland Ridge that separates the Arctic Mediterranean from the rest of the World Ocean (the shaded areas on the map are shallower than 500 m). In the upper layer warm, saline water passes the plateau on its way from the Atlantic into the Arctic Mediterranean (many thin arrows). At deeper levels, cold and less saline water flows towards the ridge to overflow it into the Atlantic (thick arrow).

The CTD-data were acquired by the Faroese research vessel R/V Magnus Heinason in the period 1987 - 1999. In this work we only use CTD observations from the four standard sections around the Faroes (Fig. 2). Some of the standard sections extend into waters well away from the Faroe Plateau, but we only use the standard stations close to the Plateau. Table 1 lists the location and number of standard stations included for each section as well as the number of cruises with complete temperature and salinity observations at each standard station.

The ADCP-data were also acquired along the four standard sections at the 12 mooring sites shown in Figure 2. Ten of these sites (Nwana, Nwnb, Nwnc, Nwnd, Nwfa, Nwfb, Nwfc, Nwsa, Nwsb, and Nwsc) were established as part of the Nordic WOCE/VEINS experiments while the remaining two (FGEB and FGEC) were funded by the “Faroese GEM” partnership of oil companies with interest in Faroese waters. Deployments and recoveries were made with R/V Magnus Heinason and data were preprocessed as described by Larsen *et al.* (1999). The current velocity data from the ADCP’s is organized into “bins”, each of which represents a horizontal layer over which the velocity is averaged. We only include deployments of more than two months duration. Table 2 lists main characteristics of the ADCP-data acquired at each site.

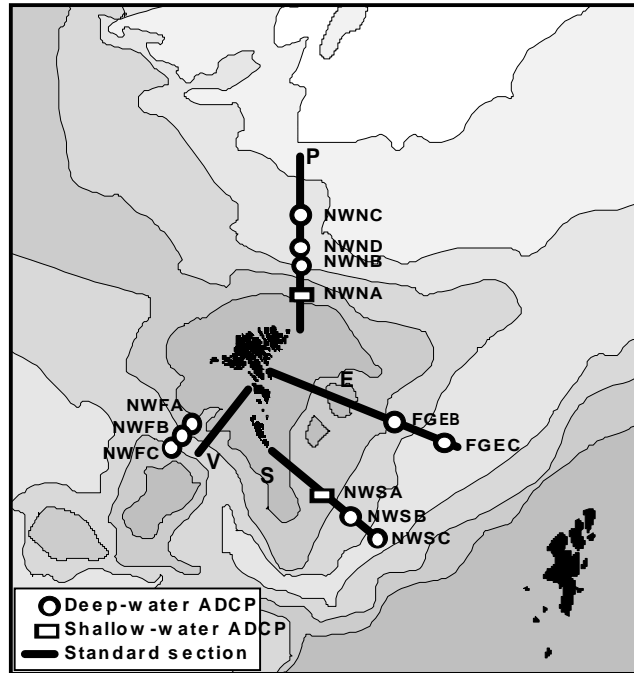


Figure 2. Thick lines indicate the four standard sections labeled N, E, S, and V. The figure shows only the part of the sections discussed in this paper. Circles show location of 75 kHz RDI Broadband ADCP’s in the top of moorings with the instrument at 600 - 800 meter depth. The two rectangles at Nwana and Nwsa indicate 150 kHz RDI Broadband ADCP’s mounted within trawproof frames on the bottom.

Table 2. Main characteristics of the ADCP deployments considered. For each site (Fig. 2) the table lists position, bottom depth, the number of deployments, the total number of days in all deployments, the typical number of bins (varies typically ± 1 bin from one deployment to another, but may vary ± 3 bins), and the typical depth range covered (varies typically ± 25 m from one deployment to another, but may vary ± 75 m).

Site	Position		Bott. depth	Number depl.	Number days	Number bins	Depth range
	Latit.	Long.					
NWFA	61°26'N	8°15'W	718m	1	71	23	126m - 676m
NWFB	61°25'N	8°17'W	816m	4	971	26	150m - 775m
NWFC	61°24'N	8°19'W	836m	1	71	24	219m - 794m
Nwana	62°42'N	6°05'W	298m	4	1182	24	50m - 280m
NWNB	62°55'N	6°05'W	943m	3	832	24	75m - 650m
NWNC	63°16'N	6°06'W	1731m	4	1170	23	75m - 625m
NWND	62°58'N	6°06'W	1283m	1	214	23	84m - 634m
NWSA	61°00'N	5°50'W	296m	3	760	24	48m - 278m
NWSB	60°47'N	5°18'W	783m	3	586	23	100m - 650m
NWSC	60°34'N	4°46'W	1067m	4	927	23	70m - 620m
FGEB	61°35'N	4°22'W	779m	1	109	23	85m - 635m
FGEC	61°33'N	4°00'W	1195m	1	109	21	146m - 646m

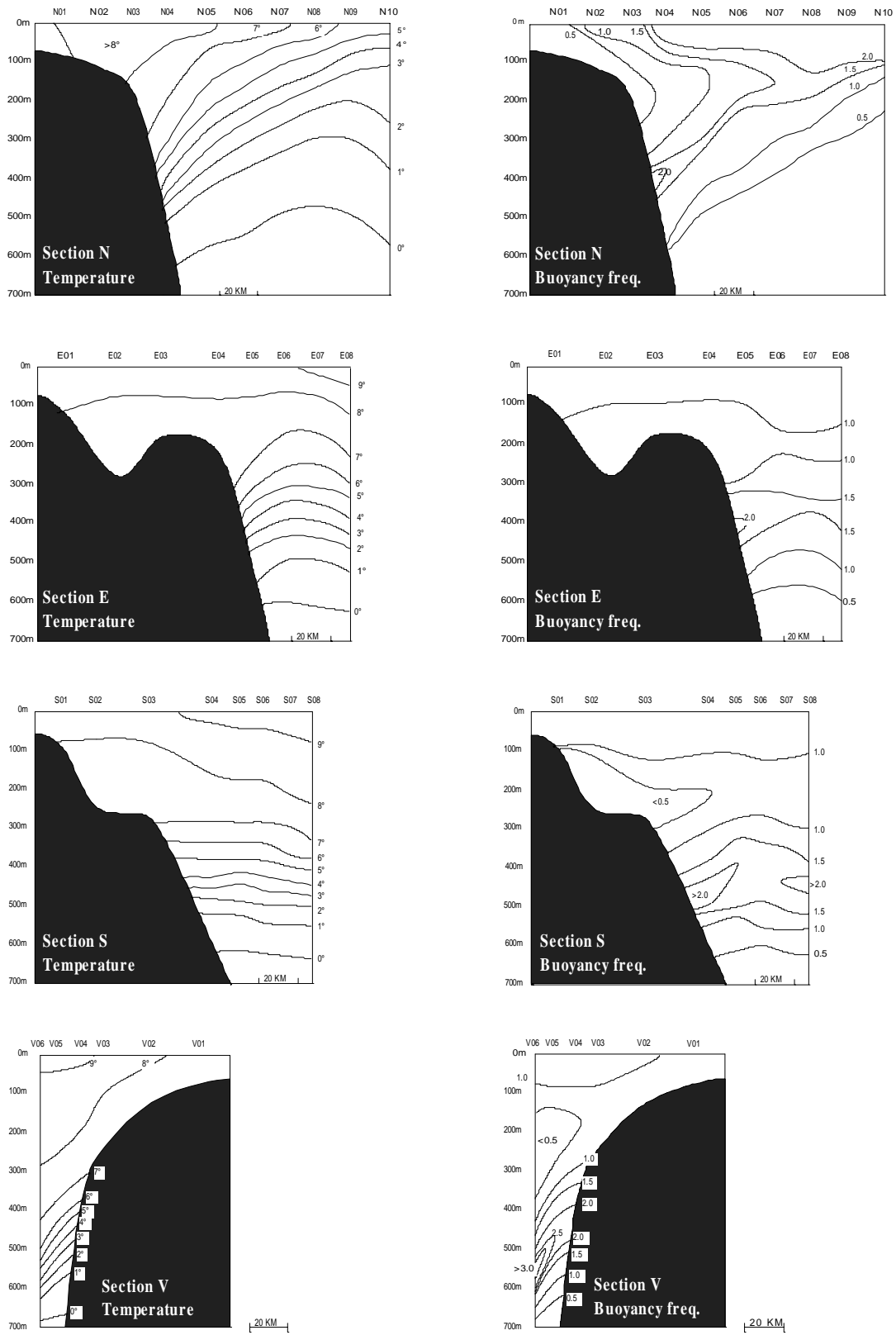


Figure 3. Average distributions of temperature and buoyancy frequency along the four standard sections shown in Figure 2.

RESULTS

Thermocline structure. Using all hydrographic cruises with both temperature and calibrated salinity observations from all included standard stations on each section (Table 1), we computed average T and S distributions on the sections and also the average distribution of buoyancy frequency (Fig.3). The depth of the pycnocline may be defined by the maximum of the B-V frequency and it is seen to descend from the surface layer in the northernmost part of section N down to about 400 m on the north Faroe slope. In the Faroe-Shetland Channel the maximum is not very sharp but is also centered around 400 m while the Faroe Bank Channel has a sharp maximum around 500 m depth.

Bottom temperature oscillations. In addition to velocity, the ADCP's record the ambient temperature at the instrument. At most of the sites, the instrument was so deep that it was well below the thermocline and also on top of a mooring where the influence of tidal currents on the mooring may induce fictitious temperature variations at the instrument. At sites NWNA and NWSA, however, the ADCP's were mounted in trawlproof frames directly on the bottom so that any observed temperature variation at tidal frequencies unambiguously can be ascribed to variations in the water close to the bottom.

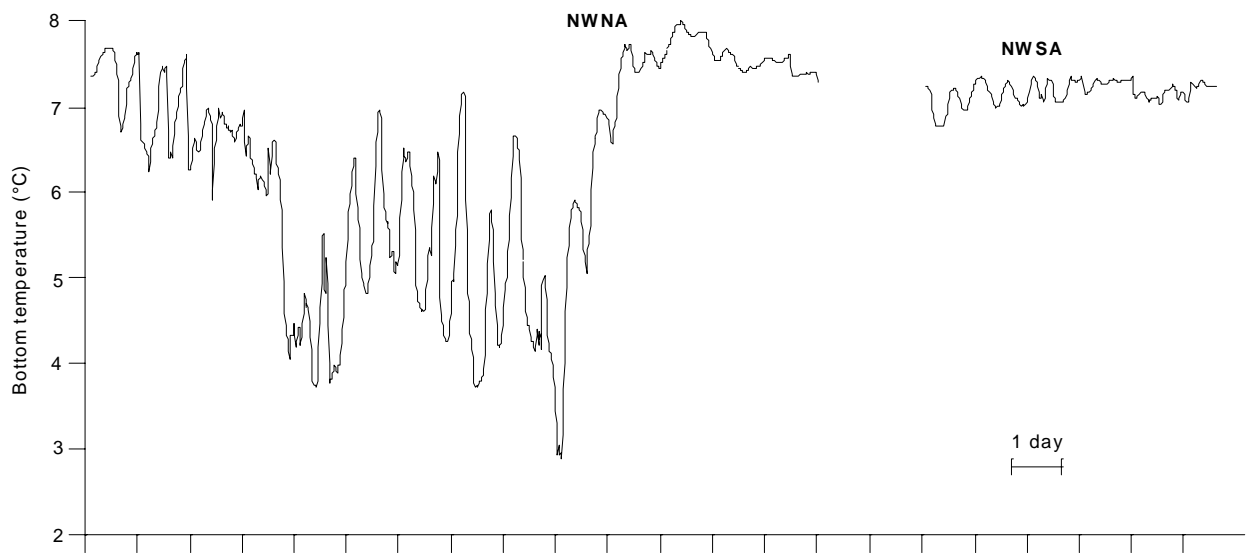


Figure 4. Examples of subseries of the bottom temperature record at NWSA and NWSA respectively which include periods with periodic oscillations.

The bottom depth at these two sites is rather too shallow in relation to the typical thermocline for us to expect a clear signal, but excerpts from the time series show that occasionally there are periodic fluctuations at both sites (Fig. 4) and averaged power spectra from these sites show distinct peaks around semidiurnal frequencies (Fig. 5). To investigate these oscillations further, we carried out a standard tidal analysis of the temperature using the Foreman package (see references).

At site NWSA, three out of the four available series (Table 2) had M_2 as the most significant constituent in the tidal frequency range (period of about a day or shorter). The Greenwich phaselags for these three series were 299° , 310° , and 315° respectively. We also analyzed 10 subseries of length from a few days up to 2 weeks which were subsampled from these four series by eye to include periods with large oscillations. 8 of these subseries had M_2 as the dominant tidal frequency and for these the Greenwich phaselags ranged from 269° to 336° . We therefore conclude that at NWSA, there is at times a periodic temperature variation phaselocked to the semidiurnal tide with a phaselag around 300° . The largest semidiurnal temperature amplitudes found in the subseries were around 0.5°C .

A similar analysis was carried out at NWSA. There, none of the analyses of the full series showed pronounced M_2 peaks, but we also analyzed 13 short subseries which had dominant M_2 peaks. Out of these subseries, 11 had phaselags in the range: 310° to 369° while the remaining two phaselags were around 140° . Thus, at NWSA there also seems to be a periodic temperature variation phaselocked to the semidiurnal tide at times, but it is less pronounced than at NWSA and perhaps with a slightly larger phaselag around 330° . The amplitudes of the semidiurnal temperature oscillations at NWSA were also smaller than at NWSA.

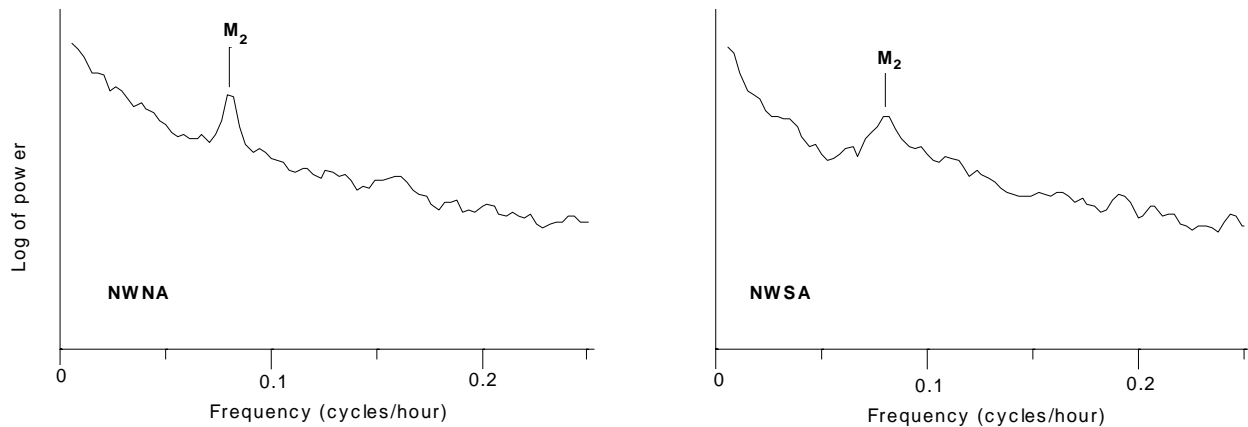


Figure 5. Power spectra of the bottom temperatures at NWNNA and NWSA computed by MATLAB and averaged over all the series.

Tidal currents. From the velocity part of the ADCP-data we have computed tidal constituents using the Foreman package, specially adapted to the ADCP observations. For each bin of each deployment this gives a set of harmonic constants describing the tidal ellipse, or alternatively amplitude and Greenwich phaselags, for each constituent included in the analysis. Figures 6, 7, 8, 9, and 10 illustrate the results for the three main semidiurnal and the two main diurnal constituents. In these figures, we have not plotted the ellipses for each bin, but rather at fixed depths with a 100 m interval where we for each series have chosen the bins that include the appropriate depth levels. To illustrate the stability of the harmonic constants, we have plotted the ellipses from different deployments at the same site and depth on top of each other, and calculated the mean and standard deviation for the phaselags.

DISCUSSION

Bottom temperature oscillations. The results from the ADCP measurements at site NWNNA and NWSA show that there are at times semidiurnal variations in the bottom temperature driven by the tide. Phaselags around 300° and 330° respectively correspond fairly well with Knudsen's (1911) cited result when the limited accuracy of both our approaches are taken into account. Knudsen (1911) argued that his observations were due to vertical motion of the thermocline, not to horizontal advection of temperature gradients past the observational site. At the bottom, vertical velocity is zero, so temperature variations must necessarily be associated with horizontal movement. Comparing the tidal temperature and velocity oscillations, we find that the temperature maxima occur when the current flows parallel to the topography, with the coast on the righthand side. The temperature thus has a maximum at the end of offshore flow.

Tidal currents. The tidal ellipses shown in Figures 6 - 10 exhibit a number of interesting features. First we note that repeated observations from the same site yield similar, but not identical, ellipses. This is the case, not only for the weaker constituents, but also for M_2 . This could be due to instrumental variation, since often different instruments have been used during repeated measurements at the same site. If this was the only explanation, then we would have expected similar or at least systematic changes with depth. Figure 11 explores this possibility in more detail for the two sites NWNNA and NWSB. At NWSB, The Greenwich phaselags seem reasonably stable, but the amplitudes, especially the amplitude of the eastward velocity component are certainly not. There is no indication, however, that this is due to variation between instruments.

Another possible explanation might be inaccuracy of the tidal analyses since the series have different lengths. Experimentation with simulated series shows, however, that this can explain only a small part of the variability of the harmonic constants. We conclude that the tidal character of the current is not stable; neither as regards amplitude nor phaselag. In Figure 11, this is most pronounced for NWNNA where the M_2 current is weak; but it is also the case for NWSB. Even though the phaselags for NWSB do not show variation from one series to another very clearly in the figure, there are differences of about 10° . We have checked whether the variations in the harmonic constants have a systematic seasonal component; but have not been able to identify any.

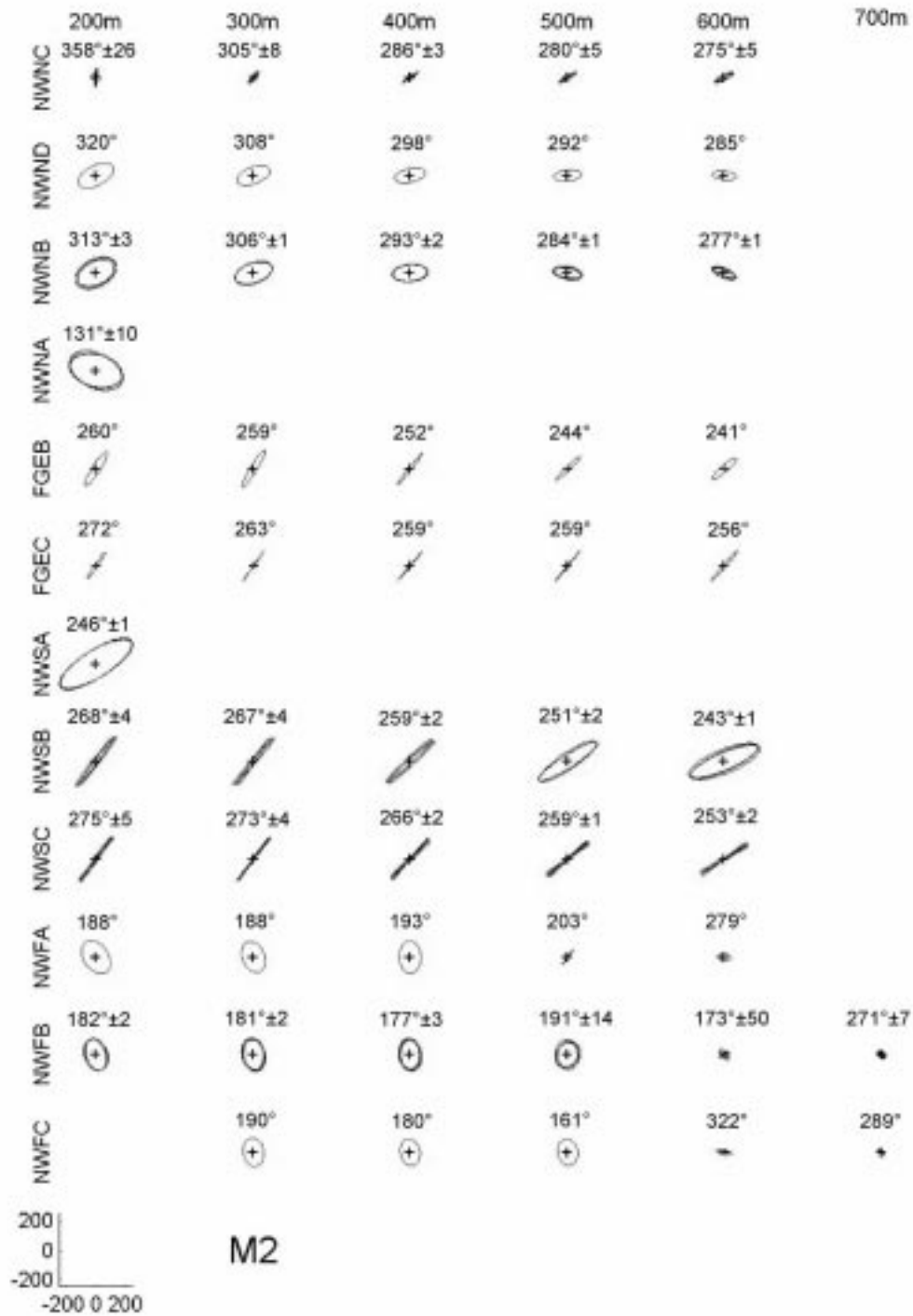


Figure 6. Tidal ellipses for the M_2 constituent plotted at fixed depths and including all deployments from each site. The velocity scale (in mm/sec) is shown in the bottom left corner of the figure and the mean phaselag (in deg.) is shown above the ellipses. A "+" in the center of the ellipses indicates anticyclonic (clockwise) rotation while cyclonic rotation is indicated by "-".



Figure 7. Tidal ellipses for the S_2 constituent plotted at fixed depths and including all deployments from each site. The velocity scale (in mm/sec) is shown in the bottom left corner of the figure and the mean phaselag (in deg.) is shown above the ellipses. A "+" in the center of the ellipses indicates anticyclonic (clockwise) rotation while cyclonic rotation is indicated by "-".



Figure 8. Tidal ellipses for the N_2 constituent plotted at fixed depths and including all deployments from each site. The velocity scale (in mm/sec) is shown in the bottom left corner of the figure and the mean phaselag (in deg.) is shown above the ellipses. A "+" in the center of the ellipses indicates anticyclonic (clockwise) rotation while cyclonic rotation is indicated by "-".



Figure 9. Tidal ellipses for the O_1 constituent plotted at fixed depths and including all deployments from each site. The velocity scale (in mm/sec) is shown in the bottom left corner of the figure and the mean phaselag (in deg.) is shown above the ellipses. A "+" in the center of the ellipses indicates anticyclonic (clockwise) rotation while cyclonic rotation is indicated by "-".



Figure 10. Tidal ellipses for the K_1 constituent plotted at fixed depths and including all deployments from each site. The velocity scale (in mm/sec) is shown in the bottom left corner of the figure and the mean phaselag (in deg.) is shown above the ellipses. A “+” in the center of the ellipses indicates anticyclonic (clockwise) rotation while cyclonic rotation is indicated by “-”.

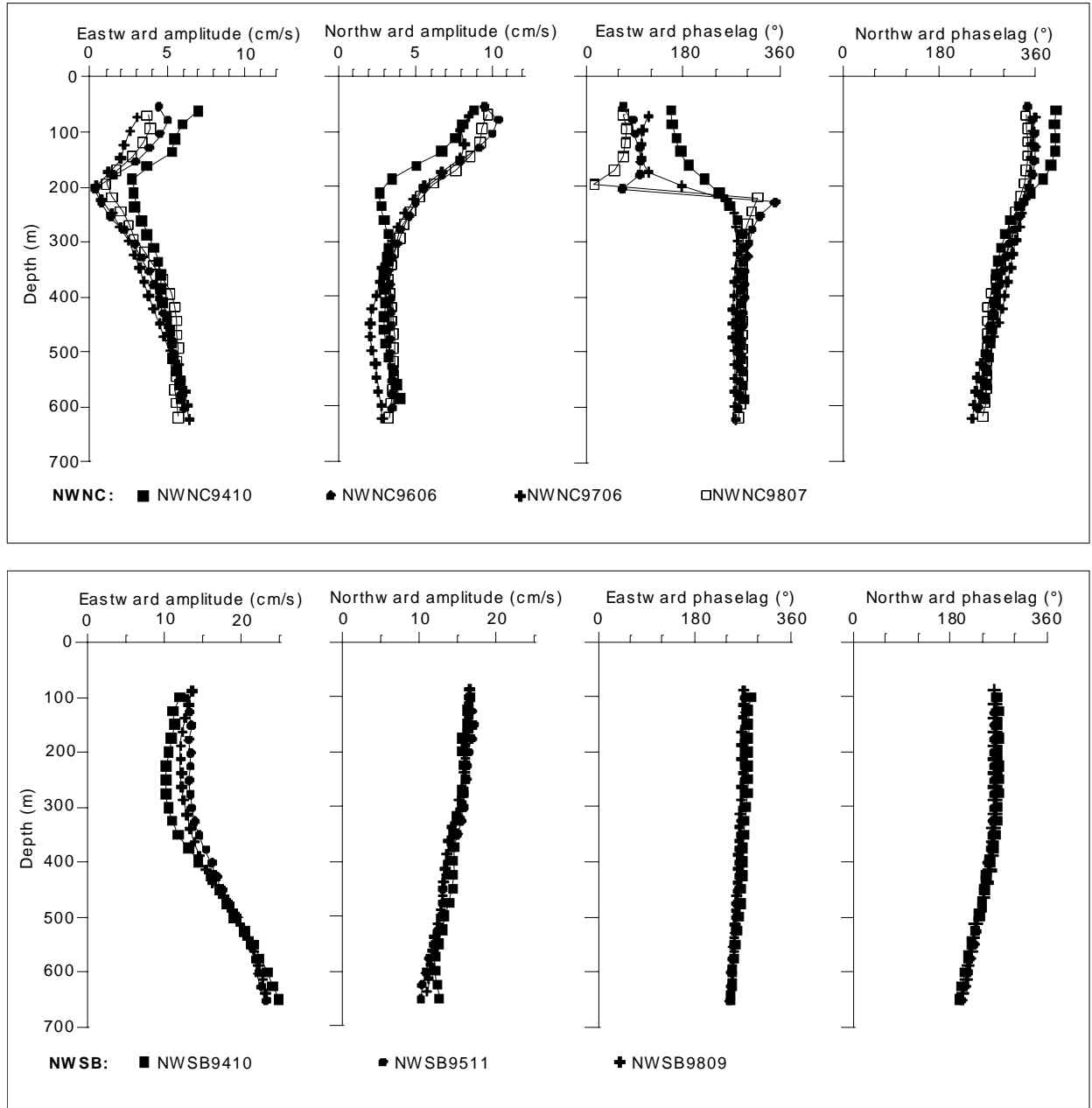


Figure 11. Changes with depth of amplitudes and Greenwich phaselags for the eastward and northward velocity components of the M_2 tide at site NWNC (upper set of graphs) and site NWSB (lower set). The results from different deployments (4 at NWNC and 3 at NWSB) are indicated by different symbols.

The variations in the harmonic constants from different series at the same site can not, however, obscure the fact that there are systematic changes both between sites and with depth. When we consider the semidiurnal tides, two facts are especially notable. One is the very weak velocities at site NWNC. Partly, this may be due to the large bottom depth at the site; but even when we scale the velocity with the depth, NWNC seems to have unusually weak flows at semidiurnal frequencies, especially for M_2 ; less so for S_2 and N_2 . This, as well as the large variation at site NWNC, previously noted, may perhaps be associated with the amphidromic system in the vicinity.

The second feature to note, is that the semidiurnal tide, especially M_2 , disappears, more or less, in the bottom of the Faroe Bank Channel, that is in the strong overflow current that brings cold water from the Norwegian Sea into

the Atlantic. This is the deepest passage between these two oceans and thus, the semidiurnal tides of the Atlantic and the Norwegian Sea do not interact directly at these depths. When we consider the diurnal tides in the Faroe Bank Channel, the situation is quite different. Both O_1 and K_1 are seen to increase in amplitude with depth and in the cold overflow water these two diurnal constituents have about the same magnitude as M_2 .

Away from the Faroe Bank Channel the semidiurnal tides exhibit a fairly consistent depth variation. From the upper layer (200 m) down below the thermocline (600 m) the axes of the ellipses turn in a clockwise direction while the Greenwich phaselags decrease in magnitude. Both changes are much more pronounced north of the Faroes than in the Faroe-Shetland Channel and apply to all three of the semidiurnal constituents considered, although less pronounced for N_2 than for the other two.

With a few exceptions, the semidiurnal tides rotate in a clockwise direction at all depths where the ellipses do not degenerate into lines and, as a whole, the semidiurnal tides around the Faroe Plateau seem to be fairly well described as a two-layer system with a continuous change from the upper to the deeper layer. The depth variation of the diurnal ellipses does not seem to fit a general system as simple as this and would appear to require a modal structure of higher order to explain the observations.

References

Knudsen, M. 1911. Danish Hydrographical Investigations at the Faroe Islands in the Spring of 1910. Meddelelser fra kommissionen for havundersøgelser, serie: hydrografi, bind 2, nr. 1.

Sherwin, T. 1995. Tidal Oscillations of the Thermocline in the Faroe-Shetland Channel. Ocean Challenge, volume 6, No. 1.

Larsen, K. M. H., Hansen, B., Kristiansen, R. 1999. Nordic WOCE ADCP Deployments 1994 – 1997. The Faroese Fisheries Laboratory. Technical Report 99-05.

Foreman, M. G. G. 1978. Manual for Tidal Currents Analysis and Prediction. Pacific Marine Science Report 78-6.